

Accepted Manuscript

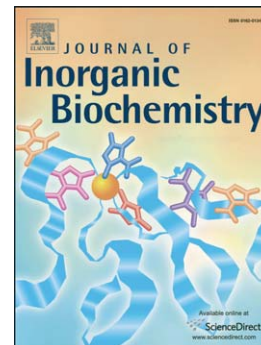
Synthesis, characterization, and binding affinity of hydrosulfide complexes of synthetic iron(II) prphyrinates

Daniel J. Meininger, Hadi D. Arman, Zachary J. Tonzetich

PII: S0162-0134(16)30241-0
DOI: doi: [10.1016/j.jinorgbio.2016.08.014](https://doi.org/10.1016/j.jinorgbio.2016.08.014)
Reference: JIB 10069

To appear in: *Journal of Inorganic Biochemistry*

Received date: 3 June 2016
Revised date: 23 August 2016
Accepted date: 25 August 2016



Please cite this article as: Daniel J. Meininger, Hadi D. Arman, Zachary J. Tonzetich, Synthesis, characterization, and binding affinity of hydrosulfide complexes of synthetic iron(II) prphyrinates, *Journal of Inorganic Biochemistry* (2016), doi: [10.1016/j.jinorgbio.2016.08.014](https://doi.org/10.1016/j.jinorgbio.2016.08.014)

This is a PDF file of an unedited manuscript that has been accepted for publication. As a service to our customers we are providing this early version of the manuscript. The manuscript will undergo copyediting, typesetting, and review of the resulting proof before it is published in its final form. Please note that during the production process errors may be discovered which could affect the content, and all legal disclaimers that apply to the journal pertain.

Synthesis, Characterization, and Binding Affinity of
Hydrosulfide Complexes of Synthetic Iron(II)
Porphyrinates

*Daniel J. Meininger, Hadi D. Arman, and Zachary J. Tonzetich**

Department of Chemistry, University of Texas at San Antonio (UTSA), San Antonio, TX 78249

*Corresponding author: zachary.tonzetich@utsa.edu, (210) 458-5465

ABSTRACT

The binding and reactivity of the hydrosulfide ion (HS^-) to iron(II) porphyrinates has been examined for several synthetic *meso*-tetraphenylporphine (TPP) derivatives. In all cases, HS^- coordinates to the iron centers in a 1:1 stoichiometry with formation constants (K_f) that reflect the electronic characteristics of the porphyrinate ligands. In the case of the F_8TPP ligand (F_8TPP = dianion of 5,10,15,20-*tetrakis*(2,6-difluorophenyl)porphine), an intermediate complex proposed as the hydrosulfide bridged dimer, $(\text{Bu}_4\text{N})[\text{Fe}_2(\mu\text{-SH})(\text{F}_8\text{TPP})_2]$, was identified by NMR spectroscopy en route to formation of $(\text{Bu}_4\text{N})[\text{Fe}(\text{SH})(\text{F}_8\text{TPP})]$. A robust procedure is reported for the synthesis and isolation of the parent hydrosulfide adduct, $(\text{Bu}_4\text{N})[\text{Fe}(\text{SH})(\text{TPP})]$, which has permitted a detailed examination of its spectroscopy and chemical reactivity. Electrochemical measurements demonstrate that $[\text{Fe}(\text{SH})(\text{TPP})]^-$ is oxidized reversibly at a potential of -0.832 V (vs ferrocene/ferrocenium) consistent with other iron porphyrinates containing sulfur-based ligands. Despite this fact, chemical oxidation of $(\text{Bu}_4\text{N})[\text{Fe}(\text{SH})(\text{TPP})]$ with ferrocenium tetrafluoroborate produced only $[\text{Fe}(\text{TPP})]$ indicating that the putative iron(III) hydrosulfide adduct, $[\text{Fe}(\text{SH})(\text{TPP})]$, decomposes rapidly. Treatment of $(\text{Bu}_4\text{N})[\text{Fe}(\text{SH})(\text{TPP})]$ with other biologically relevant molecules such as NO and 1,2-dimethylimidazole resulted in simple displacement of the HS^- ligand as governed by the relative K_f values of the added ligands. The solid-state structure of one hydrosulfide adduct, $(\text{Bu}_4\text{N})[\text{Fe}(\text{SH})(\text{F}_8\text{TPP})]$, was determined by X-ray crystallography and found to display the expected five-coordinate geometry about iron with an Fe-S distance of $2.323(1)$ Å. The relevance of the hydrosulfide chemistry with synthetic iron porphyrinates is discussed in terms of the possible reactivity for H_2S and its derivatives at heme sites in biology.

KEYWORDS: hydrogen sulfide, hydrosulfide, iron(II), heme models, porphyrins, signaling molecules

Introduction

Hydrogen sulfide continues to gain prominence as an endogenous signaling molecule in mammalian biology.[1-3] This growing interest has resulted in H₂S now being considered alongside CO and NO as a significant gaseotransmitter.[4-7] Biological processes attributed to the action of hydrogen sulfide include vasodilation,[8, 9] numerous cardiovascular effects,[10, 11] neuromodulation,[12] and cytoprotection.[13-18] Unlike CO and NO, however, the coordination chemistry of H₂S and its analogs is severely underdeveloped, especially with metal centers and ligand environments relevant to biological cofactors. Such coordination chemistry is of utmost interest since the mechanisms of action of H₂S can be envisioned to involve interactions with transition metals.

Among the multitude of sites where H₂S is believed to play a role, heme centers represent perhaps the most logical targets of metal-based reactivity.[19] Indeed, hydrogen sulfide has already been shown to interact with cytochrome oxidases,[20-22] myeloperoxidase,[23] hemoglobin and myoglobin,[24, 25] as well as other heme-containing proteins found in invertebrates.[26] Classically, the interaction of excess H₂S with both hemoglobin and myoglobin under aerobic conditions is known to involve formation of sulfhemes.[27] The sulfhemes feature a modified protoporphyrin ring that contains a dihydrothiophene unit that results from insertion of sulfur into the backbone substituents of the pyrrole group.[28-31] Binding of hydrogen sulfide to the iron center of heme proteins without modification of the porphyrin ring has also been observed in several organisms. Coordination of H₂S to the iron center of cytochrome c oxidase has been proposed as a means of inducing a hibernative state in mice,[32, 33] and binding of H₂S to Hemoglobin I of the bivalve mollusk *Lucina pectinata* is the primary means through which the clam transports the molecule for metabolism by its symbiotic

bacteria.[34-37] In all cases, model studies with synthetic iron porphyrinates would help clarify the intricacies of hydrogen sulfide coordination chemistry at heme centers.[38]

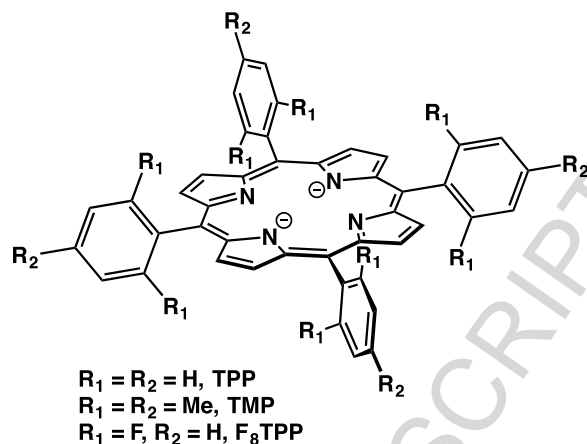
Hydrogen sulfide exists in a 3:1 ratio of $\text{HS}^-:\text{H}_2\text{S}$ at a physiological pH of 7.4 allowing for the possibility of both species to act as potential ligands.[39] Even when considering both species, however, reports of well-characterized transition metal complexes containing H_nS ($n = 1$ or 2) are rare.[40-45] Even more scarce are examples involving metalloporphyrinates. Scheidt reported an early example of a hydrosulfide complex of an iron(III) porphyrinate,[46] although later work has questioned the identity of the iron(III) species.[47] Holm has also reported observing a 5-coordinate iron(III) hydrosulfide, $[\text{Fe}(\text{SH})(\text{OEP})]$ (OEP = dianion of octaethylporphine), as an unstable intermediate during the reaction of $[\text{Fe}_2(\text{OEP})_2(\mu\text{-O})]$ with H_2S (g).[48] In similar fashion, our group identified the related species, $[\text{Fe}(\text{SH})(\text{TMP})]$ (TMP = dianion of tetramesitylporphine), upon the treatment of $[\text{Fe}(\text{OH})(\text{TMP})]\cdot\text{H}_2\text{O}$ with H_2S (g).[49] Beyond these examples from iron chemistry, we have also recently described the first example of a gallium hydrosulfide complex, $[\text{Ga}(\text{SH})(\text{TPP})]$, which serves as a structural model for the putative iron(III) species.[50] A Mn(III) example containing a related tetraazaporphyrinate ligand, $[\text{Mn}(\text{SH})(\text{OESPZ})]$ (OESPZ = dianion of *octakis*(ethylsulfanyl)tetraazaporphine), has also been reported.[51]

More recently, several groups have investigated the chemistry of synthetic iron(II) porphyrinates with the hydrosulfide ion. Scheidt's initial report in 2010 provided the first structural information and formation constants (K_f) for adducts of HS^- with iron(II) porphyrinates.[52] The work also proposed the existence of a *bis*-hydrosulfide adduct to account for changes observed in the electronic absorbance spectra during titration experiments with HS^- . Subsequent work by the groups of Coleman, Nasri, and Pluth with picket fence porphyrinates

also identified and quantified the binding of the hydrosulfide ion to iron(II).[53-55] Notably, Pluth and coworkers established that only 1:1 binding occurs with iron(II) porphyrinates and that the presence of coordinating solvents such as DMF or additional ligands such as *N*-methylimidazole does not alter the binding of the hydrosulfide ion. Furthermore, their results demonstrated that only HS⁻ and not H₂S nor S₈ is capable of binding to iron(II) porphyrinates. Work with a water-soluble model complex has generated similar results,[56] suggesting a proclivity for heme iron(II) centers to form five-coordinate adducts with the hydrosulfide ion.

Despite the growing body of literature concerning the interaction of H₂S and its derivatives with heme iron, no robust procedure for the synthesis of hydrosulfide adducts of iron(II) or iron(III) has been put forward. The ability to isolate such adducts is highly desirable, as it permits additional reactivity studies to be performed with other biologically relevant small molecules that may demonstrate important interplay with H₂S. With this motivation in mind, we have investigated the binding of HS⁻ with three synthetic iron(II) porphyrinates utilizing the TPP, TMP and F₈TPP ligands (Chart 1). Importantly, we have demonstrated that hydrosulfide adducts of these simple *meso*-tetraarylporphyrinates can be prepared in solution and even isolated in reproducible fashion for the parent ligand, TPP.

Chart 1. *meso*-Tetraarylporphyrinates used in this study.



Results and Discussion

Solution binding studies

Although the binding of the hydrosulfide ion to iron(II) porphyrins has been examined previously, no general trends have been put forward relating the formation constants to the substitution pattern about the porphyrin macrocycle. We therefore set out to repeat the binding studies of HS^- with a series of iron(II) porphyrinates containing structurally related, but electronically distinct porphyrin ligands (Chart 1). In addition, we chose to utilize the soluble, well-defined tetrabutylammonium hydrosulfide (Bu_4NSH) as the source of the HS^- ion.[57] Solutions of $[\text{Fe}(\text{TPP})]$ were titrated with Bu_4NSH in THF under the rigorous exclusion of oxygen and monitored by UV-vis spectroscopy. In contrast to previous studies, we chose to focus on spectral changes occurring in the Q-band region of the absorption spectrum. The Q-bands were selected for monitoring in this study because they appeared more sensitive to changes in hydrosulfide ligation than the Soret transition. Upon introduction of Bu_4NSH to $[\text{Fe}(\text{TPP})]$, diminution of the Q-band absorbance at 540 nm was accompanied by the growth of two new absorbances at 582 and 625 nm. This transformation is consistent with an $\text{A} \rightarrow \text{B}$ process complete with well-anchored isosbestic points (Figure 1).

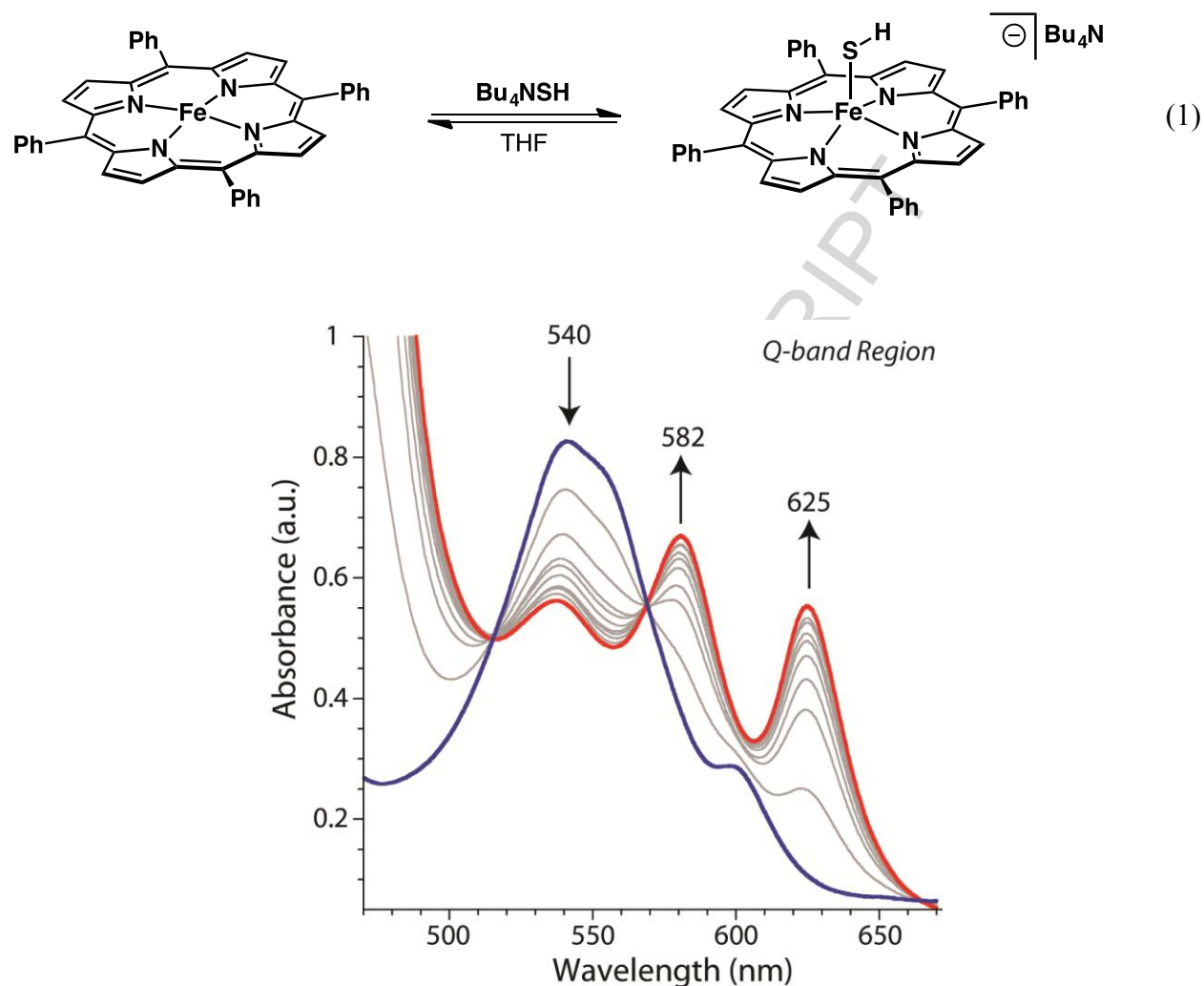


Figure 1. Electronic absorption spectrum of [Fe(TPP)] in THF (blue) showing the changes observed in the Q-band region of the spectrum upon successive addition of Bu₄NSH (gray lines represent 0.4 equivalent increments). The final spectrum (red) is that of (Bu₄N)[Fe(SH)(TPP)].

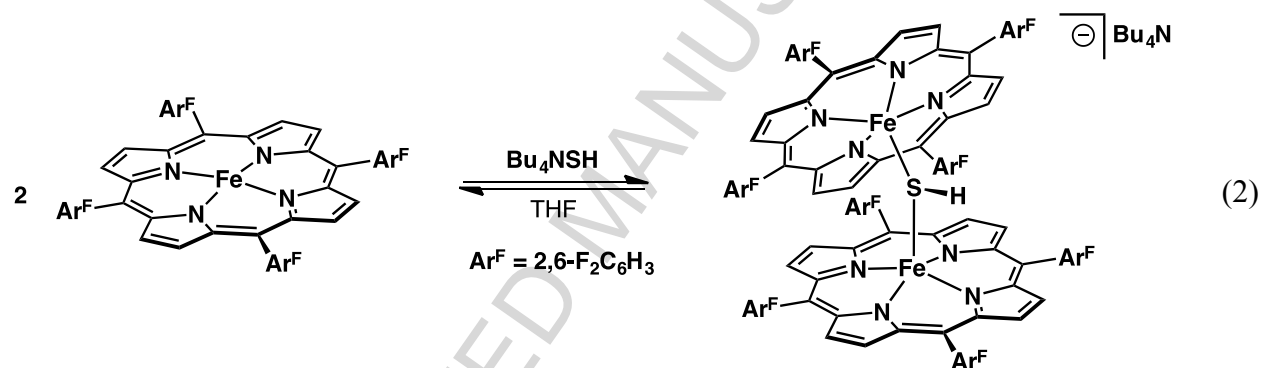
The spectroscopic changes displayed in Figure 1 are assigned to the formation of the five-coordinate adduct, (Bu₄N)[Fe(SH)(TPP)] (equation 1). Additional equivalents of Bu₄NSH did not lead to any further changes in the absorbance spectrum. The observation of new bands at 582 and 625 nm is consistent with related studies employing synthetic porphyrinates,^[52, 54] and demonstrates that the hydrosulfide ion binds to [Fe(TPP)] in a 1:1 stoichiometry. The titration data was fit to a strong binding model (see Supporting Information), yielding a log*K_f* value of 5.3(2) for an average of three experiments. This value indicates relatively strong binding of the

HS^- ion, and is comparable to the value of 4.8(2) obtained by Pluth for the *N*-methylimidazole (N-MeIm) ligated analog, $[\text{Fe}(\text{N-MeIm})_2(\text{TPP})]$.^[54] The higher value obtained in this work most likely reflects the absence of competitive binding by N-MeIm (*vide infra*).

The iron(II) complex containing tetramesitylporphyrin, $[\text{Fe}(\text{TMP})]$, was next examined to probe the effects of incorporating electron-donating groups into the *meso* substituents. Our initial hypothesis was that the more electron-rich ligand would result in weaker binding of the hydrosulfide ion as compared to $[\text{Fe}(\text{TPP})]$. Titration of $[\text{Fe}(\text{TMP})]$ with Bu_4NSH again produced changes to the electronic absorption spectrum consistent with an $\text{A} \rightarrow \text{B}$ process accompanied by spectral features resembling those observed with $[\text{Fe}(\text{TPP})]$. As predicted, a larger concentration of Bu_4NSH was required to observe complete formation of $[\text{Fe}(\text{SH})(\text{TMP})]^-$. Fitting the data to a strong binding model afforded a $\log K_f$ value of 2.6(2), substantially less than that found for $[\text{Fe}(\text{TPP})]$. Therefore, we conclude that the more electron-rich nature of $[\text{Fe}(\text{TMP})]$ results in weaker binding of HS^- .

To complement the binding studies with $[\text{Fe}(\text{TPP})]$ and $[\text{Fe}(\text{TMP})]$, we also investigated the binding of hydrosulfide to the iron(II) complex containing the electron-withdrawing F_8TPP ligand. We expected to observe higher affinity for hydrosulfide in line with the enhanced Lewis acidity of the iron center in $[\text{Fe}(\text{F}_8\text{TPP})]$ as has been observed with imidazole binding to the nitrosyl analog.^[58] In contrast to the previous titration experiments, however, the binding of HS^- to $[\text{Fe}(\text{F}_8\text{TPP})]$ was not found to follow an $\text{A} \rightarrow \text{B}$ process. Absorbance changes in THF did not resemble those observed with $[\text{Fe}(\text{TPP})]$ and $[\text{Fe}(\text{TMP})]$ until more than one equivalent of Bu_4NSH was added to $[\text{Fe}(\text{F}_8\text{TPP})]$. This behavior precluded determination of an accurate K_f value for $[\text{Fe}(\text{SH})(\text{F}_8\text{TPP})]^-$, and suggested that an intermediate species was forming prior to the five-coordinate adduct. NMR data for this intermediate species (*vide infra*) are consistent with a

bimetallic bridged-hydrosulfide species (equation 2). The formation of such a species conceivably results from the pronounced affinity of the iron(II) center in $[\text{Fe}(\text{F}_8\text{TPP})]$ for axial ligands. Capture of free $[\text{Fe}(\text{F}_8\text{TPP})]$ by sub-stoichiometric quantities of $[\text{Fe}(\text{SH})(\text{F}_8\text{TPP})]$ formed during the initial phase of the titration results in formation of the bimetallic complex. Only after addition of excess hydrosulfide does the bimetallic complex then evolve to the expected five-coordinate adduct.



In order to provide further evidence for the equilibrium in equation 2, the reaction between $[\text{Fe}(\text{F}_8\text{TPP})]$ and Bu_4NSH was followed by ^1H NMR spectroscopy. Figure 2 displays the spectral changes that accompany addition of increasing equivalents of Bu_4NSH to a solution of $[\text{Fe}(\text{F}_8\text{TPP})]$ in a mixture of benzene- d_6 and dichloromethane- d_2 . As is clear from the spectra, a new species with a pyrrolic resonance at 37 ppm appears immediately upon addition of 0.5 equivalents of Bu_4NSH . This species continues to gain intensity until it maximizes at 2 equivalents of added Bu_4NSH . At this point, resonances for $[\text{Fe}(\text{F}_8\text{TPP})]$ are no longer apparent. Upon addition of further equivalents of Bu_4NSH , a new pyrrolic resonance at 54 ppm appears. The downfield resonance at 54 ppm is consistent with the five-coordinate adduct, $[\text{Fe}(\text{SH})(\text{F}_8\text{TPP})]^-$, and its sequential formation supports the proposal that the species at 37 ppm corresponds to an intermediate. The remaining spectral features of the intermediate species are

consistent with a five-coordinate complex (*vide infra*) leading us to favor its formulation as $[\text{Fe}_2(\mu\text{-SH})(\text{F}_8\text{TPP})_2]^-$.

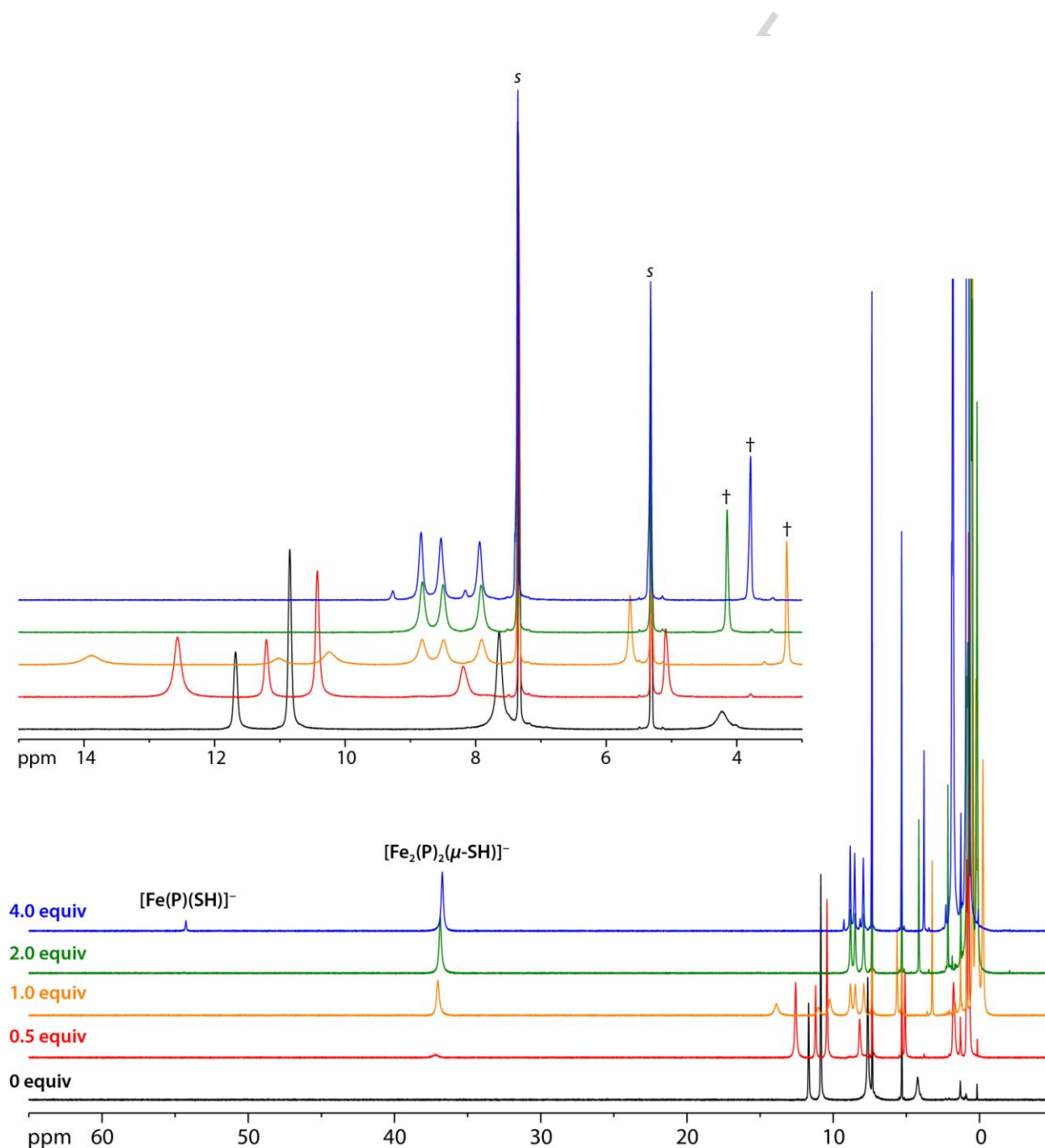


Figure 2. 500 MHz ^1H NMR spectra resulting from the successive addition of Bu_4NSH to $[\text{Fe}(\text{F}_8\text{TPP})]\cdot\text{THF}$ in a mixture of benzene- $d_6(s)$ and dichloromethane- $d_2(s)$. Inset displays an expanded view of the region between 3 and 15 ppm. Crosses denote resonances due to THF.

Results from binding studies with the three iron(II) porphyrinate species demonstrate that electronic effects from the porphyrin ligand can influence the thermodynamics of hydrosulfide coordination. Electron-withdrawing porphyrin ligands appear to increase the affinity for HS^- as evidenced by the observation of the putative bimetallic species $[\text{Fe}_2(\mu\text{-SH})(\text{F}_8\text{TPP})_2]^-$ (Equation 2). Formation constants for $[\text{Fe}(\text{SH})(\text{TPP})]^-$ and $[\text{Fe}(\text{SH})(\text{TMP})]^-$ determined in the present study are displayed in Table 1 along with results from previous studies. Also included in Table 1 are $\log K_f$ values for other small molecule ligands relevant to the biological chemistry of heme centers. These data demonstrate that the hydrosulfide ion binds to iron(II) centers with an affinity comparable to that of carbon monoxide and imidazole.

Table 1. Formation constants (in $\log K_f$ form) for hydrosulfide and other adducts of iron(II) porphyrinates.

Complex	$\log K_f$	Reference
$[\text{Fe}(\text{SH})(\text{TPP})]^-$	5.3(2)	This work
$[\text{Fe}(\text{SH})(\text{TPP})]^-$	4.8(2) ^a	54
$[\text{Fe}(\text{SH})(\text{TMP})]^-$	2.6(2)	This work
$[\text{Fe}(\text{SH})(\text{TMP})]^-$	4.6(7)	52
$[\text{Fe}(\text{SH})(\text{TAP})]^-$	4.7(4)	52
$[\text{Fe}(\text{SH})(\text{OEP})]^-$	5.0(2)	52
HbI-SH from <i>L. pectinata</i>	4.7	37
HS-hemeCD3	4.9	56
$[\text{Fe}(\text{NO})(\text{TPP})]$	>9 ^b	[59]
$[\text{Fe}(\text{CO})(\text{TPP})]$	4.83(2)	[60]
$[\text{Fe}(\mathbf{1,2}\text{-Me}_2\text{Im})(\text{TPP})]$	4.43(5)	[61]

^aPrepared from $[\text{Fe}(\text{N-MeIm})_2(\text{TPP})]$. ^bValue estimated from the rate constant for the forward reaction of $[\text{Fe}(\text{TPP})]$ with $\text{NO}(\text{g})$.

Preparation, isolation, and characterization of hydrosulfide adducts

Having quantified the binding of HS^- to several iron(II) porphyrinates, we next sought to isolate and fully characterize the hydrosulfide adducts. Scheidt has reported the isolation and solid state structure of several $[\text{Fe}(\text{SH})(\text{P})]^-$ species, however, these compounds required extended crystallization times to afford solid material, and were paired with the somewhat inconvenient cation, $[\text{Na}(222)]^+$ (222 = Kryptofix-222).[52] We were therefore motivated to develop a straightforward, robust preparative procedure for complexes of the type $(\text{Bu}_4\text{N})[\text{Fe}(\text{SH})(\text{P})]$. Gratifyingly, we found that treatment of $[\text{Fe}(\text{TPP})]$ with an excess of Bu_4NSH (~4 equivalents) afforded the desired hydrosulfide complex in yields of up to 90% after crystallization from a mixture of benzene and pentane. ^1H NMR spectra of isolated $(\text{Bu}_4\text{N})[\text{Fe}(\text{SH})(\text{TPP})]$ in benzene- d_6 display a resonance for the pyrrolic hydrogen atoms near 59 ppm, consistent with a five-coordinate high-spin iron(II) porphyrinate (see Supporting Information).[54] Resonances for the hydrogen atoms of the Bu_4N^+ cation are located at negative chemical shift values, indicating tight ion pairing with the paramagnetic iron complex in benzene. Spectra recorded in acetonitrile- d_3 display similar chemical shift values for the $[\text{Fe}(\text{SH})(\text{TPP})]^-$ anion, however the hydrogen atoms of the Bu_4N^+ cation now appear closer to their range in diamagnetic salts demonstrating that weaker ion pairing occurs in more polar solvents. The resonance for the hydrogen atom of the coordinated HS^- ligand cannot be observed by ^1H NMR nor can a fundamental for the S-H stretch be identified by infrared spectroscopy. Attempts to subject crystals of $(\text{Bu}_4\text{N})[\text{Fe}(\text{SH})(\text{TPP})]$ to X-ray diffraction experiments produced data that was too poor for high quality refinement. Nonetheless, the connectivity of the atoms within crystals of $(\text{Bu}_4\text{N})[\text{Fe}(\text{SH})(\text{TPP})]\cdot 2\text{C}_6\text{H}_6$ could be established unambiguously and confirmed the molecular structure (see Supporting Information).

Preparation of the hydrosulfide adducts containing the TMP and F₈TPP ligands proved more challenging than that of TPP. Formation of Bu₄N[Fe(SH)(TMP)] was verified by ¹H NMR spectroscopy in acetonitrile from the reaction of [Fe(TMP)] with 2.5 equivalents of Bu₄N₃SH (see Supporting Information). Isolation of pure (Bu₄N)[Fe(SH)(TMP)], however, was unsuccessful most likely as a consequence of the weaker binding affinity of hydrosulfide to [Fe(TMP)] (Table 1). Attempts to crystallize the material resulted in recovery of Bu₄N₃SH and [Fe(TMP)].

In the case of [Fe(F₈TPP)], we first targeted the putative bimetallic species, (Bu₄N)[Fe₂(μ-SH)(F₈TPP)₂]. Addition of Bu₄N₃SH to [Fe(F₈TPP)] in several organic solvents demonstrated that dichloromethane gave the highest yields of the bimetallic species (Figure 2). Reactions conducted in THF or acetonitrile lead primarily to formation of the monometallic adduct, (Bu₄N)[Fe(SH)(F₈TPP)], perhaps as a consequence of weaker ion pairing. Accordingly, we were able to isolate (Bu₄N)[Fe₂(μ-SH)(F₈TPP)₂] from reactions in dichloromethane employing 1.5 equivalents of Bu₄N₃SH. Material obtained from these conditions displayed relatively clean ¹H and ¹⁹F NMR spectra consistent with a five-coordinate species (see Supporting Information). For example, inequivalent resonances for the *meta*-hydrogen atoms of the *meso*-difluorophenyl rings were apparent, as were two distinct resonances for the *ortho*-fluorine atoms. The monometallic complex, Bu₄N[Fe(SH)(F₈TPP)], could be obtained using 2 or more equivalents of Bu₄N₃SH in THF or acetonitrile. The NMR and UV-vis features of the complex were very similar to those of [Fe(SH)(TPP)]⁻ and [Fe(SH)(TMP)]⁻ (see Supporting Information).

Attempts to grow crystals of (Bu₄N)[Fe₂(μ-SH)(F₈TPP)₂] from mixtures of dichloromethane and pentane suitable for X-ray diffraction resulted in crystals of the monometallic adduct, (Bu₄N)[Fe(SH)(F₈TPP)]·3CH₂Cl₂. The structure of (Bu₄N)[Fe(SH)(F₈TPP)] is displayed in Figure 3. The Fe(1)-S(1) distance of 2.3229(10) Å is comparable to the value of 2.3887(13) Å

reported by Scheidt for $[\text{Na}(222)][\text{Fe}(\text{SH})(\text{TAP})]$.^[52] The slightly contracted Fe-S bond length is consistent with the more electron-withdrawing nature of F_8TPP ligand. The closest contacts between the Bu_4N^+ cation and the iron complex occur between S(1) and the hydrogen atoms connected to C(49) (2.630 Å) and C(53) (2.754 Å). There is also a short contact of 2.557 Å between the hydrogen atom of a co-crystallized dichloromethane molecule and S(1), suggesting the presence of hydrogen bonding in the crystal (see Supporting Information). The remaining metric parameters of note (see caption to Figure 3) are in line with those of other five-coordinate iron(II) porphyrinates.^[62]

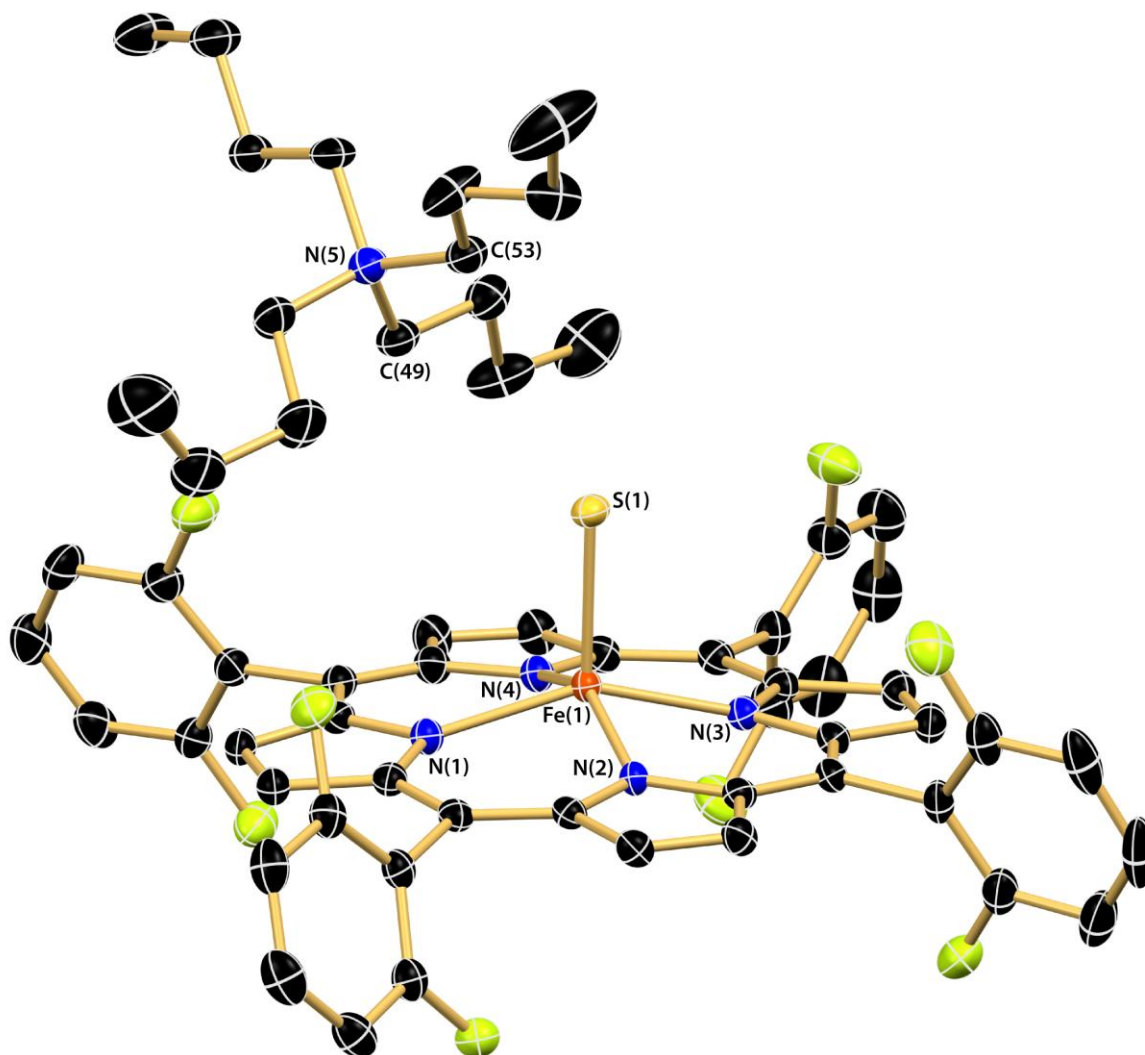


Figure 3. Thermal ellipsoid (50%) rendering of the solid-state structure of $(\text{Bu}_4\text{N})[\text{Fe}(\text{SH})(\text{F}_8\text{TPP})]$. Hydrogen atoms and co-crystallized molecules of CH_2Cl_2 omitted for clarity. Selected bond distances (\AA) and angles (deg): $\text{Fe}(1)\text{-S}(1) = 2.3229(10)$, $\text{Fe}(1)\text{-N}_{\text{avg}} = 2.114(3)$, $\Delta N_4 = 0.525(4)$, $(\text{N-Fe-N})_{\text{avg}} = 86.46(11)$.

Electrochemistry of $(\text{Bu}_4\text{N})[\text{Fe}(\text{SH})(\text{TPP})]$

Successful isolation of $(\text{Bu}_4\text{N})[\text{Fe}(\text{SH})(\text{TPP})]$ afforded the opportunity to examine its electrochemistry. Of particular interest is the position of the iron(II)/iron(III) couple, which gives information about the reductive stability of the corresponding iron(III) hydrosulfide. The cyclic voltammogram of $(\text{Bu}_4\text{N})[\text{Fe}(\text{SH})(\text{TPP})]$ in dichloromethane is displayed in Figure 4. The complex shows a reversible $\text{Fe}^{\text{II/III}}$ couple centered at -0.832 V versus ferrocene/ferrocenium. This value is surprisingly high (more positive) given the relatively low $\text{p}K_a$ of H_2S . For comparison, the $\text{Fe}^{\text{II/III}}$ couple for $[\text{Fe}(\text{SSi}^i\text{Pr}_3)(\text{TPP})]$, which bears the more electron-donating silanethiolate ligand, is found at -1.15 V.[49] The relatively high potential for the $\text{Fe}^{\text{II/III}}$ couple of $(\text{Bu}_4\text{N})[\text{Fe}(\text{SH})(\text{TPP})]$ indicates that the corresponding iron(III) hydrosulfide complex, $[\text{Fe}(\text{SH})(\text{TPP})]$, is more thermodynamically unstable with respect to reduction than iron(III) porphyrinates containing thiolate ligands. This fact, coupled with the likely kinetic instability of $[\text{Fe}(\text{SH})(\text{TPP})]$ attributable to the small size of the HS^- ligand, explains why prior attempts to prepare the iron(III) hydrosulfide complex by ourselves and others have resulted in reduction to iron(II). Despite this apparent instability, evidence with heme proteins suggests that the Fe(III) oxidation state may play an important role in the binding of the hydrosulfide ion in vivo.[38]

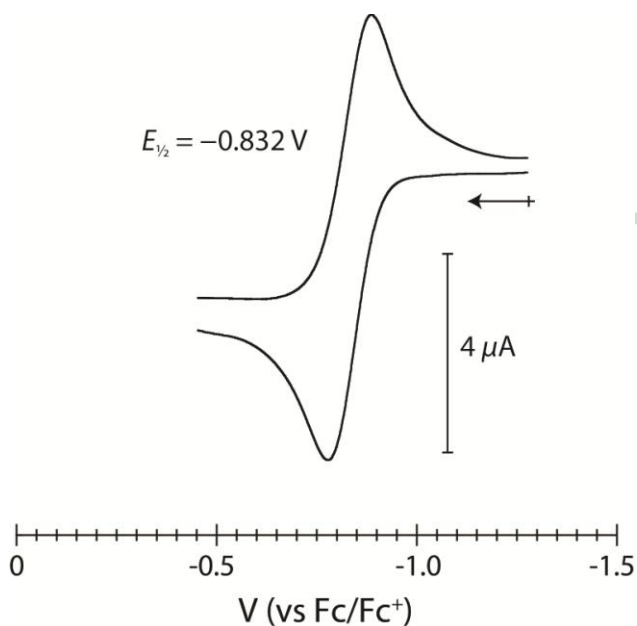
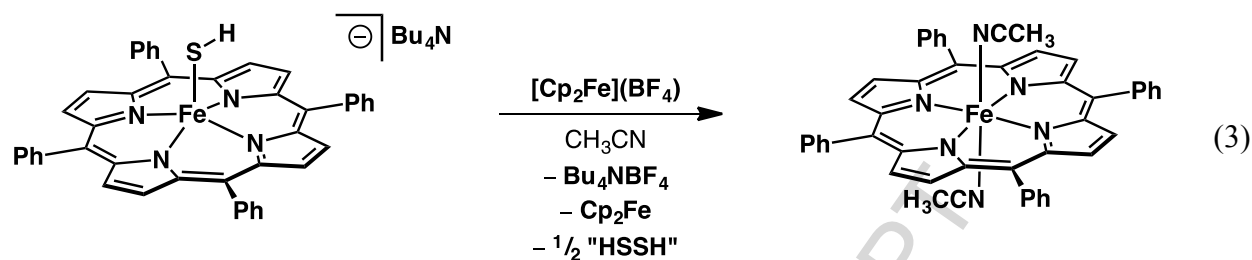


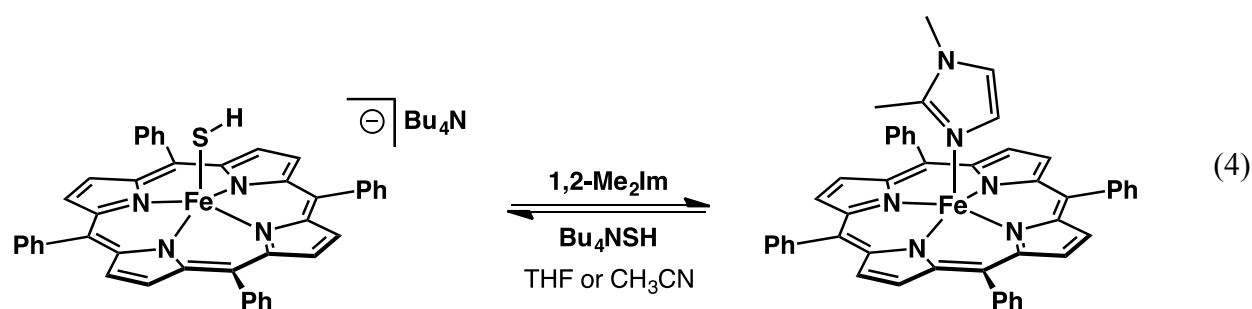
Figure 4. Region of the cyclic voltammogram of $(\text{Bu}_4\text{N})[\text{Fe}(\text{SH})(\text{TPP})]$ displaying the reversible iron(II)/iron(III) couple. Experiment was performed at a Pt disk electrode in dichloromethane at 50 mV/s scan rate with 0.1 M Bu_4NPF_6 as supporting electrolyte.

Reaction chemistry

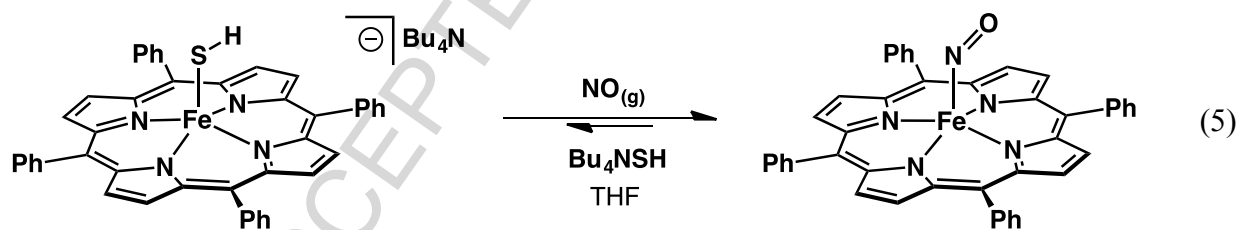
As a final component to our investigations of hydrosulfide adducts of iron(II) porphyrinates we surveyed the reaction chemistry of $(\text{Bu}_4\text{N})[\text{Fe}(\text{SH})(\text{TPP})]$ with a series of biologically-relevant small molecules. We first examined the one-electron oxidation of $(\text{Bu}_4\text{N})[\text{Fe}(\text{SH})(\text{TPP})]$ using $[\text{Cp}_2\text{Fe}](\text{BF}_4)$ (equation 3). The reaction was carried out at low concentrations to deter the potential for bimolecular decomposition of a putative iron(III) hydrosulfide species. At concentrations of 8 or 80 μM , addition of $[\text{Cp}_2\text{Fe}](\text{BF}_4)$ to $(\text{Bu}_4\text{N})[\text{Fe}(\text{SH})(\text{TPP})]$ in acetonitrile resulted in immediate formation of the iron(II) complex, $[\text{Fe}(\text{NCCH}_3)_2(\text{TPP})]$ as judged by UV-vis spectroscopy. This result is consistent with prior attempts to isolate a hydrosulfide complex of an iron(III) porphyrinate and confirms the instability of putative $[\text{Fe}(\text{SH})(\text{TPP})]$. [48, 49] The fate of the hydrosulfide ligand is not known at this time, but disulfide or persulfide species such as HSSH are likely involved in the iron(III) reduction process. [63]



In an effort to create a model for a heme site containing both hydrosulfide and histidine coordination, we next examined the reaction of $(\text{Bu}_4\text{N})[\text{Fe}(\text{SH})(\text{TPP})]$ with 1,2-dimethylimidazole (1,2-Me₂Im). 1,2-Me₂Im was selected for its inability to form a six-coordinate bis-imidazole adduct as can be observed with *N*-methylimidazole.[64] Upon addition of 1,2-Me₂Im to solutions of $(\text{Bu}_4\text{N})[\text{Fe}(\text{SH})(\text{TPP})]$ in tetrahydrofuran or acetonitrile, no evidence was found for formation of a six-coordinate complex of the form $(\text{Bu}_4\text{N})[\text{Fe}(\text{SH})(1,2\text{-Me}_2\text{Im})(\text{TPP})]$ by either NMR or UV-vis spectroscopy (see Supporting Information). Instead, 1,2-Me₂Im was found to partially displace the hydrosulfide ligand. This behavior is consistent with establishment of an equilibrium between two five-coordinate adducts as shown in equation 4. The position of this equilibrium is determined by the relative binding affinities of the HS⁻ and 1,2-Me₂Im ligands (Table 1). Consistent with this proposal, addition of a large excess of 1,2-Me₂Im to $(\text{Bu}_4\text{N})[\text{Fe}(\text{SH})(\text{TPP})]$ resulted in complete formation of $[\text{Fe}(1,2\text{-Me}_2\text{Im})(\text{TPP})]$.



The interplay of H₂S and nitric oxide has been proposed to result in formation of other biologically important small molecules such as HSNO.[65] In order to assay the potential for such reactivity with (Bu₄N)[Fe(SH)(TPP)], we turned our attention to nitric oxide. Introduction of 1 atm of NO(g) to a solution of (Bu₄N)[Fe(SH)(TPP)] in benzene-*d*₆ was found to lead to complete consumption of the hydrosulfide complex and formation of the ferrous nitrosyl, [Fe(NO)(TPP)], as judged by ¹H NMR spectroscopy. This finding is not surprising given the affinities of hydrosulfide versus nitric oxide (Table 1). Examining the reverse reaction, addition of large excesses of Bu₄NSH (>20 equivalents) to [Fe(NO)(TPP)] in THF was found to result in UV-vis signatures consistent with (Bu₄N)[Fe(SH)(TPP)]. Therefore, the chemistry between NO and [Fe(SH)(TPP)]⁻ is best regarded as an equilibrium that lies almost entirely toward the nitrosyl (equation 5).



Conclusions

In this contribution, we have described the synthesis, reactivity, and binding behavior of several hydrosulfide adducts of the type [Fe(SH)(P)]⁻ (P = *meso*-tetraarylporphyrinate). The structural and spectroscopic features of each complex are consistent with five-coordinate high-spin iron(II) centers. The binding affinities of HS⁻ to the different iron(II) porphyrinates reflect the electronic properties of the ligand and demonstrate that substituents on the *meso*-aryl rings of the porphyrin can play an important role in shaping the thermodynamics of hydrosulfide

coordination. This fact was most apparent for the electron-withdrawing F₈TPP ligand, where an intermediate species assigned as [Fe₂(μ-SH)(F₈TPP)₂]⁻ was detected en route to [Fe(SH)(F₈TPP)]⁻. Thus, we expect that subtle effects such as heme pocket polarity and peripheral interactions with surrounding amino acid residues may be important components of the interaction between hydrosulfide and heme proteins in biological systems.

Experimental

General Comments. Unless otherwise noted, all manipulations were performed under an atmosphere of nitrogen gas using standard Schlenk techniques or in a Vacuum Atmospheres glovebox. Tetrahydrofuran, diethyl ether, pentane, dichloromethane, and toluene were purified by sparging with argon and passage through two columns packed with 4 Å molecular sieves. Benzene-*d*₆ was dried over sodium ketyl and vacuum-distilled prior to use. Dichloromethane-*d*₂ and acetonitrile-*d*₃ were sparged with nitrogen and stored over 4 Å molecular sieves prior to use. ¹H NMR spectra were recorded on Varian spectrometer operating at 500 MHz (¹H) and referenced to the residual protium resonance of the solvent. ¹⁹F NMR spectra were obtained on the same spectrometer at 470 MHz and referenced externally to 1,2-difluorotetrachloroethane (δ = -67.80 ppm vs CFCl₃). UV-vis spectra were recorded on a Cary-60 spectrophotometer in air-tight Teflon-capped quartz cells. Cyclic voltammetry was performed at 23 °C on a CH Instruments 620D electrochemical workstation. A 3-electrode set-up was employed comprising a 1 mm platinum disk working electrode, a platinum wire auxiliary electrode, and a Ag/AgCl quasi-reference electrode. Triply recrystallized Bu₄NPF₆ was used as the supporting electrolyte. All electrochemical data were referenced internally to the ferrocene/ferrocenium couple at 0.00 V. Elemental analyses were performed by the CENTC Elemental Analysis Facility at the University of Rochester.

Materials. Metalloporphyrins [Fe^{II}(TPP)], [Fe^{II}(TMP)], and [Fe^{II}(F₈TPP)] were prepared by literature procedures or slight modifications thereof.[66, 67] In most cases, the iron(II) porphyrinates contained residual THF, which was quantified by ¹H NMR spectroscopy and accounted for in subsequent spectroscopic experiments. Bu₄NSH was prepared as published.[57] NO gas was purified by bubbling through 10 M NaOH (*aq*) then collected from the headspace of the solution. Ferrocenium tetrafluoroborate and 1,2-dimethylimidazole were purchased from commercial suppliers and used as received.

X-ray Crystallography. Crystals suitable for X-ray diffraction were mounted in Paratone oil onto a glass fiber and frozen under a nitrogen cold stream. The data were collected at 98(2) K using a Rigaku AFC12/Saturn 724 CCD fitted with Mo K α radiation ($\lambda = 0.71073$ Å). Data collection and unit cell refinement were performed using Crystal Clear software.[68] Data processing and absorption correction, giving minimum and maximum transmission factors, were accomplished with Crystal Clear and ABSCOR,[69] respectively. All structures were solved by direct methods and refined on F^2 using full-matrix, least-squares techniques with SHELXL-97.[70] All carbon bound hydrogen atom positions were determined by geometry and refined by a riding model. The position of the sulfur-bound hydrogen atom in (Bu₄N)[Fe(SH)(F₈TPP)] could not be identified from the electron density map and was not included in the structure refinement.

(Bu₄N)[Fe(SH)(TPP)]. To 5 mL of THF was added 25.9 mg (38.7 μ mol) of [Fe^{II}(TPP)] and 46 mg (170 μ mol, 4.3 equivalents) of Bu₄NSH. The solution was stirred for 12 hrs at 23 °C during which time the dark red solution acquired a green tint. The THF was evacuated under reduced pressure and the remaining residue was extracted into 5 mL of toluene and filtered to remove excess Bu₄NSH. The toluene solution was then concentrated to dryness and the crude compound

crystallized from a 2:1 mixture of benzene and pentane at ambient temperature to afford the desired compound as 32.9 mg (90%) of dark red-green needles. Note that failure to crystallize the crude product results in a tar like substance that is difficult to work with. $^1\text{H NMR}(\text{C}_6\text{D}_6)$: δ 59.1 (8 pyr-*H*), 11.3 (4 *o*-Ar*H*), 9.0 (4 *m*-Ar*H*), 8.0 (4 *o*-Ar*H*), 7.8 (4 *m*-Ar*H*), 7.7 (4 *p*-Ar*H*), -0.75 (12 Bu₄N-CH₃), -1.5 (8 Bu₄N-CH₂), -4.2 (8 Bu₄N-CH₂), -7.2 (8 Bu₄N-CH₂). UV-vis λ_{max} , nm (ϵ , M⁻¹ cm⁻¹): 415 (122,000), 451 (49,000), 537 (6700), 582 (8100), 625 (6800). Anal. Calc. for C₆₀H₆₅FeN₅S·H₂O: C, 74.90; H, 7.02; N, 7.28. Found: C, 74.52; H, 7.24; N, 7.07.

(Bu₄N)[Fe(SH)(TMP)]. To 3 mL of THF was added 26.1 mg (31.2 μmol) of [Fe^{II}(TMP)] and 19.9 mg (72.2 μmol , 2.3 equivalents) of Bu₄NSH. The solution was stirred for 12 hrs at 23 °C after which time the THF was evacuated to dryness affording the crude compound in essentially quantitative recovery as a red solid containing excess Bu₄NSH. $^1\text{H NMR}(\text{CD}_3\text{CN})$: δ 54.15 (8 pyr-*H*), 9.23 (4 *m*-Ar*H*), 8.36 (4 *m*-Ar*H*), 4.40 (12 *o*-CH₃), 3.23 (12 *p*-CH₃), 3.08 (Bu₄N-CH₂), 1.83 (8 *o*-CH₃), 1.60 (Bu₄N-CH₂), 1.35 (Bu₄N-CH₂), 0.97 (Bu₄N-CH₃). UV-vis λ_{max} , nm (ϵ , M⁻¹ cm⁻¹): 416 (114,000), 455 (40,600), 538 (6800), 583 (7300), 627 (5400).

(Bu₄N)[Fe(SH)(F₈TPP)]. To 5 mL of THF was added 25.3 mg (31.1 μmol) of [Fe^{II}(F₈TPP)] and 17.6 mg (63.9 μmol , 2.1 equivalents) of BU₄NSH. The solution was stirred for 12 hrs at 23 °C. Pentane was added to the THF solution to precipitate the desired compound in essentially quantitative recovery as a crude solid containing excess Bu₄NSH. Crystals suitable for X-ray diffraction were grown by vapor diffusion of pentane into a saturated CH₂Cl₂ solution of the complex. $^1\text{H NMR}(\text{CD}_3\text{CN})$: δ 56.91 (8 pyr-*H*), 9.36 (4 *m*-Ar*H*), 8.57 (4 *m*-Ar*H*), 8.31 (4 *p*-Ar*H*), 2.81 (BU₄N-CH₂), 1.38 (BU₄N-CH₂), 1.20 (BU₄N-CH₂), 0.89 (BU₄N-CH₃). UV-vis λ_{max} , nm (ϵ , M⁻¹ cm⁻¹): 412 (111,000), 450 (35,300), 537 (8900), 572 (8600), 614 (3700).

(Bu₄N)[(Fe₂(μ -SH)(F₈TPP)₂]. To 5 mL of CH₂Cl₂ was added 24.9 mg (30.6 μ mol) of [Fe(F₈TPP)] and 12.4 mg (45.0 μ mol, 1.5 equivalents) of Bu₄NSH. The solution was stirred for 12 hrs at 23 °C, after which time the CH₂Cl₂ was evacuated to dryness to afford the crude product in essentially quantitative recovery as a red solid. ¹H NMR(CD₂Cl₂): δ 36.8 (pyr-*H*), 8.8 (*m*-Ar*H*), 8.5 (*m*-Ar*H*), 7.9 (*p*-Ar*H*), 0.13 (Bu₄N-CH₃), -0.50 (Bu₄N-CH₂), -1.3 (Bu₄N-CH₂), -1.7 (Bu₄N-CH₂). ¹⁹F NMR(CD₂Cl₂): -98.0, -101.7.

Binding Studies. All binding studies were performed in anhydrous, deoxygenated THF. In the case of [Fe(TMP)] toluene was used to prepare initial stock solutions of the metal complex due to solubility issues with THF. Subsequent dilutions were performed with THF to ensure that the presence of small amounts of toluene was negligible. The presence of even trace amounts of oxygen was found to lead to irreproducible results due to competitive oxidation of iron(II). This precaution was most important for experiments with [Fe(TMP)], which is highly susceptible to oxidation. Solutions of iron(II) porphyrinates were prepared at concentrations around 85 μ M to give appropriate absorbances for peaks in the *Q*-band region. Stock solutions of Bu₄NSH in THF were prepared such that 1.0 mL portions corresponded to 0.40 equivalents or 1.0 equivalents per iron center. Solutions of the iron porphyrinate and Bu₄NSH were combined in a 10.0 mL volumetric flasks and brought to volume with THF to ensure that all titration points contained the same concentration of iron. The mixture of iron porphyrinate and Bu₄NSH was allowed to stand for 5 minutes in the glovebox prior to sampling to ensure that equilibrium had been established. The sample was then transferred to an air-tight cuvette and sealed with a Teflon cap before bringing outside the glovebox for analysis by UV-vis spectroscopy. Formation constants were determined from a strong binding model by fitting the titration data using KaleidaGraph (see Supporting Information).

TABLE OF ABBREVIATIONS

TPP - *meso*-tetraphenylporphyrinate
TMP - *meso*-tetramesitylporphyrinate
F₈TPP - *meso*-tetrakis-(2,6-difluorophenyl)porphyrinate
TAP - *meso*-tetrakis-(4-anisyl)porphyrinate
OEP - octaethylporphyrinate
1,2-Me₂Im - 1,2-dimethylimidazole.

Supporting Information. Additional spectra, figures, and crystallographic information including crystallographic information files (in .cif format).

Author Contributions

The manuscript was written through contributions of all authors. All authors have given approval to the final version of the manuscript.

ACKNOWLEDGMENT

The authors thank the Welch Foundation (AX-1772) for financial support of this work. The CENTC Elemental Analysis Facility is supported by NSF (CHE- 0650456).

REFERENCES

- [1] L. Li, P. Rose, P.K. Moore, *Annu. Rev. Pharmacol. Toxicol.* 51 (2011) 169-187.
- [2] R. Banerjee, *Antiox. Redox Signal.* 15 (2011) 339-341.
- [3] R. Wang, *Physiol. Rev.* 92 (2012) 791-896.
- [4] R. Wang, *FASEB J.* 16 (2002) 1792-1798.
- [5] C. Mancuso, P. Navarra, P. Preziosi, *J. Neurochem.* 113 (2010) 563-575.
- [6] R.A. Decreau, J.P. Collman, *Front. Physiol.* 6 (2015)
- [7] M. Kajimura, R. Fukuda, R.M. Bateman, T. Yamamoto, M. Suematsu, *Antioxid. Redox Signal.* 13 (2010) 157-192.
- [8] G. Yang, L. Wu, B. Jiang, W. Yang, J. Qi, K. Cao, Q. Meng, A.K. Mustafa, W. Mu, S. Zhang, S.H. Snyder, R. Wang, *Science* 322 (2008) 587-590.
- [9] W. Zhao, J. Zhang, Y. Lu, R. Wang, *EMBO J.* 20 (2001) 6008-6016.
- [10] Y.-H. Liu, M. Lu, L.-F. Hu, P.T.H. Wong, G.D. Webb, J.-S. Bian, *Antioxid. Redox Signal.* 17 (2012) 141-185.
- [11] N. Skovgaard, A. Goulliaev, M. Aalling, U. Simonsen, *Curr. Pharm. Biotechnol.* 12 (2011) 1385-1393.
- [12] H. Kimura, *Mol. Neurobiol.* 26 (2002) 13-19.
- [13] M. Whiteman, P.K. Moore, *J. Cell. Mol. Med.* 13 (2009) 488-507.
- [14] J. Biermann, W.A. Lagrèze, N. Schallner, C.I. Schwer, U. Goebel, *Mol. Vis.* 17 (2011) 1275-1286.
- [15] S. Shi, Q.-s. Li, H. Li, L. Zhang, M. Xu, J.-l. Cheng, C.-h. Peng, C.-q. Xu, Y. Tian, *Cell Biol. Int.* 33 (2009) 1095-1101.

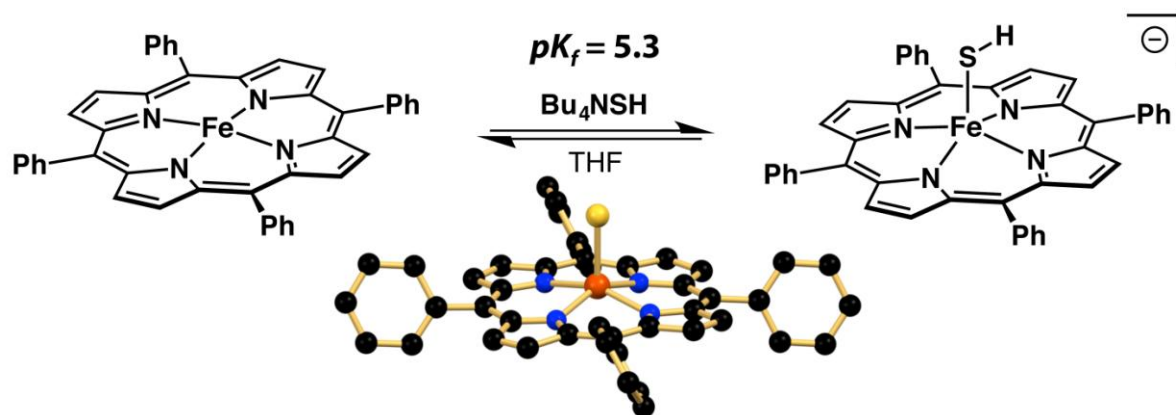
- [16] Y.-Y.P. Mok, M.S. Bin Mohammed Atan, C.Y. Ping, W.Z. Jing, M. Bhatia, S. Moochhala, P.K. Moore, *Br. J. Pharmacol.* 143 (2004) 881-889.
- [17] N.R. Sodha, R.T. Clements, J. Feng, Y. Liu, C. Bianchi, E.M. Horvath, C. Szabo, F.W. Sellke, *Eur. J. Cardio-Thorac.* 33 (2008) 906-913.
- [18] G.K. Kolluru, X. Shen, S.C. Bir, C.G. Kevil, *Nitric Oxide* 35 (2013) 5-20.
- [19] R. Pietri, E. Roman-Morales, J. López-Garriga, *Antiox. Redox Signal.* 15 (2011) 393-404.
- [20] C. Cooper, G. Brown, *J. Bioenerg. Biomembr.* 40 (2008) 533-539.
- [21] M.A. Eghbal, P.S. Pennefather, P.J. O'Brien, *Toxicology* 203 (2004) 69-76.
- [22] D.C. Dorman, F.J.M. Moulin, B.E. McManus, K.C. Mahle, R.A. James, M.F. Struve, *Toxicol. Sci.* 65 (2002) 18-25.
- [23] Z. Palinkas, P.G. Furtmueller, A. Nagy, C. Jakopitsch, K.F. Pirker, M. Magierowski, K. Jasnó, J.L. Wallace, C. Obinger, P. Nagy, *Br. J. Pharmacol.* 172 (2015) 1516-1532.
- [24] F.P. Nicoletti, A. Comandini, A. Bonamore, L. Boechi, F.M. Boubeta, A. Feis, G. Smulevich, A. Boffi, *Biochemistry* 49 (2010) 2269-2278.
- [25] M. Strianese, F. De Martino, C. Pellicchia, G. Ruggiero, S. D'Auria, *Protein Pept. Lett.* 18 (2011) 282-286.
- [26] C. Ramos-Alvarez, B.-K. Yoo, R. Pietri, I. Lamarre, J.-L. Martin, J. Lopez-Garriga, M. Negreire, *Biochemistry* 52 (2013) 7007-7021.
- [27] E. Román-Morales, R. Pietri, B. Ramos-Santana, S.N. Vinogradov, A. Lewis-Ballester, J. López-Garriga, *Biochem. Biophys. Res. Commun.* 400 (2010) 489-492.
- [28] S.V. Evans, B.P. Sishta, A.G. Mauk, G.D. Brayer, *Proc. Natl. Acad. Sci. U.S.A.* 91 (1994) 4723-4726.
- [29] J.A. Berzofsky, J. Peisach, B.L. Horecker, *J. Biol. Chem.* 247 (1972) 3783-3791.

- [30] J.A. Berzofsky, J. Peisach, W.E. Blumberg, *J. Biol. Chem.* 246 (1971) 7366-&.
- [31] J.A. Berzofsky, J. Peisach, W.E. Blumberg, *J. Biol. Chem.* 246 (1971) 3367-3377.
- [32] E. Blackstone, M. Morrison, M.B. Roth, *Science* 308 (2005) 518-518.
- [33] J.P. Collman, S. Ghosh, A. Dey, R.A. Decréau, *Proc. Natl. Acad. Sci. U.S.A.* 106 (2009) 22090-22095.
- [34] J.F. Cerda-Colón, E. Silfa, J. López-Garriga, *J. Am. Chem. Soc.* 120 (1998) 9312-9317.
- [35] M. Rizzi, J.B. Wittenberg, A. Coda, M. Fasano, P. Ascenzi, M. Bolognesi, *J. Mol. Biol.* 244 (1994) 86-99.
- [36] D.W. Kraus, J.B. Wittenberg, J.F. Lu, J. Peisach, *J. Biol. Chem.* 265 (1990) 16054-16059.
- [37] D.W. Kraus, J.B. Wittenberg, *J. Biol. Chem.* 265 (1990) 16043-16053.
- [38] S.A. Bieza, F. Boubeta, A. Feis, G. Smulevich, D.A. Estrin, L. Boechi, S.E. Bari, *Inorg. Chem.* 54 (2015) 527-533.
- [39] R.O. Beauchamp, J.S. Bus, J.A. Popp, C.J. Boreiko, D.A. Andjelkovich, P. Leber, *CRC Cr. Rev. Toxicol.* 13 (1984) 25-97.
- [40] S. Kuwata, M. Hidai, *Coord. Chem. Rev.* 213 (2001) 211-305.
- [41] C.-C. Tsou, W.-C. Chiu, C.-H. Ke, J.-C. Tsai, Y.-M. Wang, M.-H. Chiang, W.-F. Liaw, *J. Am. Chem. Soc.* 136 (2014) 9424-9433.
- [42] S. Mirra, S. Milione, M. Strianese, C. Pellecchia, *Eur. J. Inorg. Chem.* 2015 (2015) 2272-2276.
- [43] D.S. Salnikov, P.N. Kucherenko, I.A. Dereven'kov, S.V. Makarov, R. van Eldik, *Eur. J. Inorg. Chem.* 2014 (2014) 852-862.
- [44] E. Galardon, T. Roger, P. Deschamps, P. Roussel, A. Tomas, I. Artaud, *Inorg. Chem.* 51 (2012) 10068-10070.

- [45] M. Strianese, S. Mirra, V. Bertolasi, S. Milione, C. Pellecchia, *New J. Chem.* 39 (2015) 4093-4099.
- [46] D.R. English, D.N. Hendrickson, K.S. Suslick, C.W. Eigenbrot, W.R. Scheidt, *J. Am. Chem. Soc.* 106 (1984) 7258-7259.
- [47] A.L. Balch, C.R. Cornman, N. Safari, L. Latos-Grazynski, *Organometallics* 9 (1990) 2420-2421.
- [48] L. Cai, R.H. Holm, *J. Am. Chem. Soc.* 116 (1994) 7177-7188.
- [49] D.J. Meininger, J.D. Caranto, H.D. Arman, Z.J. Tonzetich, *Inorg. Chem.* 52 (2013) 12468-12476.
- [50] D.J. Meininger, M. Chee-Garza, H.D. Arman, Z.J. Tonzetich, *Inorg. Chem.* 55 (2016) 2421-2426.
- [51] G. Ricciardi, A. Bencini, S. Belviso, A. Bavoso, F. Lelj, *J. Chem. Soc., Dalton Trans.* (1998) 1985-1992.
- [52] J.W. Pavlik, B.C. Noll, A.G. Oliver, C.E. Schulz, W.R. Scheidt, *Inorg. Chem.* 49 (2010) 1017-1026.
- [53] J.P. Collman, S. Ghosh, *Inorg. Chem.* 49 (2010) 5798-5810.
- [54] M.D. Hartle, J.S. Prell, M.D. Pluth, *Dalton Trans.* 45 (2016) 4843-4853.
- [55] M. Dhifet, M.S. Belkhiria, J.C. Daran, H. Nasri, *Acta Crystallogr., Sect. E: Struct. Rep. Online* 65 (2009) m967-m968.
- [56] K. Watanabe, T. Suzuki, H. Kitagishi, K. Kano, *Chem. Commun.* 51 (2015) 4059-4061.
- [57] M.D. Hartle, D.J. Meininger, L.N. Zakharov, Z.J. Tonzetich, M.D. Pluth, *Dalton Trans.* 44 (2015) 19782-19785.
- [58] V.K.K. Praneeth, C. Näther, G. Peters, N. Lehnert, *Inorg. Chem.* 45 (2006) 2795-2811.

- [59] M. Hoshino, M. Kogure, *J. Phys. Chem.* 93 (1989) 5478-5484.
- [60] B.B. Wayland, L.F. Mehne, J. Swartz, *J. Am. Chem. Soc.* 100 (1978) 2379-2383.
- [61] T. Hashimoto, J.E. Baldwin, F. Basolo, R.L. Dyer, M.J. Crossley, *J. Am. Chem. Soc.* 104 (1982) 2101-2109.
- [62] C. Hu, C.E. Schulz, W.R. Scheidt, *Dalton Trans.* 44 (2015) 18301-18310.
- [63] T. Bostelaar, V. Vitvitsky, J. Kumutima, B.E. Lewis, P.K. Yadav, T.C. Brunold, M. Filipovic, N. Lehnert, T.L. Stemmler, R. Banerjee, *J. Am. Chem. Soc.* 138 (2016) 8476-8488.
- [64] N.J. Silvernail, A. Roth, C.E. Schulz, B.C. Noll, W.R. Scheidt, *J. Am. Chem. Soc.* 127 (2005) 14422-14433.
- [65] J.L. Miljkovic, I. Kenkel, I. Ivanović-Burmazović, M.R. Filipovic, *Angew. Chem. Int. Ed.* 52 (2013) 12061-12064.
- [66] A.D. Adler, F.R. Longo, F. Kampas, J. Kim, *J. Inorg. Nucl. Chem.* 32 (1970) 2443-2445.
- [67] C. Hu, B.C. Noll, C.E. Schulz, W.R. Scheidt, *Inorg. Chem.* 46 (2007) 619-621.
- [68] Crystal Clear, Rigaku/MSI Inc., Rigaku Corporation, The Woodlands, TX (2005).
- [69] ABSCOR, Higashi, Rigaku Corporation, Tokyo, Japan (1995).
- [70] G.M. Sheldrick, *Acta Crystallogr., Sect. A* A64 (2008) 112-122.

TOC GRAPHIC



The binding and reactivity of hydrosulfide complexes of iron(II) porphyrins is described.

Synthesis, Characterization, and Binding Affinity of Hydrosulfide Complexes of Synthetic Iron(II) Porphyrinates

*Daniel J. Meininger, Hadi D. Arman, and Zachary J. Tonzetich**

Department of Chemistry, University of Texas at San Antonio (UTSA), San Antonio, TX 78249

Highlights

- Binding constants of HS^- to several iron(II) porphyrinates are quantified.
- A robust synthetic procedure for a hydrosulfide complex is reported.
- Reactivity of the HS^- complex with biologically-relevant small molecules.
- A unique hydrosulfide-bridged diiron porphyrinate is described.